A simplified method to evaluate restoring force characteristics of reactor buildings

T.Okada
Institute of Industrial Science, University of Tokyo, Japan
K.Akino & T.Ogata
Nuclear Power Engineering Test Center, Tokyo, Japan

ABSTRACT

This paper is to propose a discrete beam model analysis to evaluate the non-linear restoring force characteristics of reinforced concrete nuclear reactor buildings macroscopically for the seismic design. In this method, overall deformation of each component such as wall or slab is considered to consist of shearing deformation and bending deformation. A rotational deformation of wall due to the elongation and slip of reinforcing bars from foundation is also considered. Each deformation is evaluated by a discrete beam model based on the non-linear stress-strain relationship estimated by the test results. Examples of verification studies to compare the computed results and the test results on the component scaled models and the scaled reactor building models are also described.

1 INTRODUCTION

Earthquake response analysis should be performed in the seismic design of reactor buildings of nuclear power plants to confirm seismic safety. In the analysis, it is important to estimate the restoring force characteristics of the structures accurately. The Finite Element Method (FEM) would be one of the most rigorous methods for this purpose. However, in order to understand the overall behavior of the structures, a simplified method is also required in the structural design of nuclear power plants.

In order to investigate the restoring force characteristics using the scaled models on PWR and BWR types of reactor buildings, Nuclear Power Engineering Test Center (NUPEC) carried out small-sized and partial model tests (Akino et al. 1982), composite model tests (Akino et al. 1984), and scale effect tests (Okada et al. 1986), and reported the outline of test results and the results of analyses by FEM (Akino et al. 1987).

In this paper, a simplified method to evaluate the restoring force characteristics of reactor buildings, developed in performing the above-mentioned studies, is described.

2 DISCRETE BEAM MODEL ANALYSIS

2.1 Outline of the method

A component model consists of discrete elements sliced perpendicular to the longitudinal axis as shown in Fig. 1. Computational flow of the total deformation is shown in Fig. 2. It is assumed that the total deformation (δ_T) at the loading position can be determined by the sum of shearing deformation (δ_S), bending deformation (δ_F), and rotational deformation (δ_θ) due to the elongation and slip of reinforcing bars from foundation. Shearing deformation of each sliced element (δ_{Si}) is determined by the skelton curve of shear stress-strain relationship ($\tau - \gamma$ relationship) as shown in Fig. 3. Bending deformation of each sliced element (δ_{Fi}) is determined by the skelton curve of moment-curvature relationship ($M - \phi$ relationship) as shown in Fig. 4, by assuming the linear distribution of strain in the element cross section.

Rotational deformation (δ_θ) is determined by the skelton curve of the base moment-rotational angle relationship ($M_b - \theta$ relationship) as shown in Fig. 5. In the case of the BWR type, the slab is also considered as a structural component and the non-linear $M - \theta$ relationship shown in Fig. 6 is considered. Shearing and axial deformations of the slab are considered having linear characteristics.

Overall behavior of the structure consisting of the components is estimated by the consideration of the compatibility and equilibrium conditions.

2.2 Estimation of skelton curve of sliced element of shear wall

Skelton curve of sliced element of shear wall was determined by the test results on 25 specimens shown in Table 1 (Akino et al. 1982) and the past research results. The test specimens consist of box wall, cylindrical wall, truncated conical wall, and octagonal tube wall, which are principal shear wall elements of a reactor building.

A trial to separate the total deformations obtained by the model tests into the shearing deformations and bending deformations was done as shown in Fig. 7. First, the bending deformation was defined using the curvature estimated by the measured vertical displacements at the both extreme ends. Then, the shearing deformation was defined by deducting the bending deformation from the total deformation.

It was found that the rotational deformation at the base (element of i=1 in Fig. 7) due to the elongation and slip of reinforcing bars from the foundation was included in the estimated bending deformation. Therefore, this was evaluated by the $M_b - \theta$ relationship independently from the bending deformation of the wall.

2.2.1 Shearing deformation

The $\tau - \gamma$ relationship is approximated by the bi-linear model with two particular points of shear cracking point and ultimate point as shown in Fig. 3. Each point is determined by the following formulas (Umemura 1980, Yoshizaki et al. 1983); In calculating the shearing deformation, the shear stress (τ) is computed form the shear force (Q) divided by the effective shear area of web (A_W).

- Shear cracking point : $\tau_1 = \sqrt{\sqrt{F_c}(\sqrt{F_c} + \sigma_V)}$, $\gamma_1 = \tau_1 / {}_cG$
- Ultimate point : $\tau_2 = [1 - \tau_s/(4.5\sqrt{F_c})] \cdot \tau_0 + \tau_s$ (provided that $\tau_s < 4.5\sqrt{F_c}$)
  $= 4.5\sqrt{F_c}$ (provided that $\tau_s \geq 4.5\sqrt{F_c}$)

  $\gamma_2 = 4 \times 10^{-3}$ (for box wall)*, 6×10^{-3} (other than box wall)*

where,
$\tau_0 =$ $(3 - 1.8 \cdot M/QD)\sqrt{F_c}$ (M/QD = 1, when M/QD > 1) (kg/cm^2)
$\tau_s =$ $(P_V + P_H) \cdot {}_s\sigma_y/2 + (\sigma_V + \sigma_H)/2$ (kg/cm^2)
F_c : compressive strength of concrete (kg/cm^2)
${}_cG$: shear modulus of concrete (= ${}_cE/[2(1+\mu)]$) (kg/cm^2)
${}_cE$: Young's modulus of concrete (kg/cm^2)
μ : Poisson's ratio
M/QD : shear span ratio
P_V, P_H : reinforcement ratios in vertical and horizontal directions
${}_s\sigma_y$: yielding stress of reinforcing bar (kg/cm^2)
σ_V, σ_H : axial stresses in vertical and horizontal directions (kg/cm^2)
* : tentatively determined values

2.2.2 Bending deformation

The $M - \phi$ relationship is approximated by the tri-linear model shown in Fig. 4 determined by the following formulas;

- Flexural cracking point : $M_1 = Z_e(1.2\sqrt{F_c} + \sigma_V)$, $\phi_1 = M_1/({}_cE \cdot I_e)$
- Flexural yielding point : $M_2 = M_y$, $\phi_2 = a/D$
- Ultimate point : $M_3 = M_u$, $\phi_3 = b/D$

where,
I_e : moment of inertia of the cross section considering reinforcements (cm^4)
Z_e : section modulus considering reinforcements (cm^3)
M_y : moment when strain of tensile reinforcement reaches yielding strain (kg·cm)
M_u : full plastic moment (kg·cm)
ϕ_2 : curvature at yielding stage (1/cm)
ϕ_3 : curvature at ultimate stage (1/cm)
D : center-to-center distance between flanges (cm)
a : assumed 0.003
b : assumed 0.12

2.2.3 Rotational deformation

Estimating the rotational deformation, it may be considered that reinforcement is extended out from the foundation as shown in Fig. 8. The real $M_b - \theta$ relationship may be shown in Fig. 5. However, the linear model as shown in Fig. 5 is adopted for the simplicity (Inada et al. 1984).

$$K_\theta = M_y/\theta_y = M_y \cdot j_y/S_y = M_y \cdot j_y/[c \cdot (40d) \cdot {}_s\epsilon_y]$$

where,
K_θ : stiffness for rotational deformation (kg·cm/rad)
θ_y : rotational angle at yielding stage ($= S_y/j_y$)
j_y = $D - X_{ny}$ (cm)
X_{ny} : distance from compression flange center to neutral axis at yielding of tensile reinforcement (cm)
S_y : amount of elongation of reinforcing bar (cm)
d : normal diameter of reinforcing bar (cm)
${}_s\epsilon_y$: yielding strain of reinforcement
c : coefficient determined by strain distribution of embedded reinforcement at yielding stage, and here, proposed as 0.64 from the test data

2.2.4 Comparison with the test values

Examples of the comparison between the test values (Akino et al. 1982) and the computed values by the discrete beam model for the $Q - \delta_T$ relationship at the loading position are shown in Fig. 9. The computed values agree well with the test values, and the appropriateness of the skelton curves in 2.2.1 to 2.2.3 is verified.

3 APPLICATION TO THE COMPOSITE MODELS

The method described previously was applied to the composite models on PWR and BWR types of nuclear reactor buildings (Akino et al. 1984). Comparison studies between the discrete beam model analysis, the model test, and the FEM analysis (Akino et al. 1987) were made, and the applicability of the discrete beam model analysis was examined. An example for the PWR type is described here. The configuration of the composite model specimen is shown in Fig. 10. The model represents the inner concrete structure of the containment vessel. The analysis was performed using a model dividing the specimen into 54 elements, with the skelton curves described in the section 2.2.

Comparisons between the computed values, the test values, and the FEM analysis values for the $Q - \delta_T$

relationship at the upper loading slab are shown in Fig. 11. The shearing deformation was computed using the effective shear area of web (A_W) as shown in Fig. 12. It can be seen that the computed values for the initial stiffness and stiffness in the inelastic range after cracking are slightly higher than both the test values and the FEM analysis values, but ultimate strengths correspond well.

4 CONCLUSION

A simplified method for macroscopical analysis of the skelton curve for the $Q - \delta_T$ relationship of a complex structure with a large amount of reinforcement such as a reactor building has been proposed.

Applying the method to the composite models, it was found that there were good correspondence with the test values, and the applicability of this method was verified.

ACKNOWLEDGEMENTS

This test has been carried out as the research project sponsored by the Ministry of International Trade and Industry in Japan. This work was performed by "Sub-committee of Restoring Force Characteristics" under "Committee of Seismic Verification Test" of NUPEC. The authors wish to acknowledge to the valuable cooperation and suggestions given by the members of the Committees.

REFERENCES

Akino, K., et al. 1982. Model Tests for Evaluation of Restoring Force Characteristics of Reactor Buildings. Summaries of Technical Papers of the Architectural Institute of Japan. : 957-970 (in Japanese).

Akino, K., et al. 1984. Model Tests for Evaluation of Restoring Force Characteristics of Reactor Buildings. Summaries of Technical Papers of the Architectural Institute of Japan. : 2331-2338 (in Japanese).

Akino, K., Suzuki, S. & Uchiyama, Y. 1987. Model Tests and Numerical Analysis on Restoring Force Characteristics of Reactor Buildings. Trans. of the 9th SMIRT Conference, K10/6, Lausanne.

Inada, Y., Ogawa, S. & Saruta, M. 1984. Study on Restoring Force Characteristics of Box-Type Shear Wall of Reactor Building. 6th Annual Research Presentation Meeting on Concrete Engineering. : 753-756 (in Japanese).

Okada, T., et al. 1986. Model Tests for Evaluation of Restoring Force Characteristics of Reactor Buildings: Part 6 Scale Effect Test. Summaries of Technical Papers of the Architectural Institute of Japan. : 1089-1090 (in Japanese).

Umemura, H. (ed.) 1980. Dynamic Earthquake-Resistant Design Method for Reinforced Concrete Buildings, p.322-324. Tokyo: Gihodo (in Japanese).

Yoshizaki, S., Ezaki, T., Korenaga, T. & Sotomura, K. 1983. Shear Strength of Shear Walls with Numerous Small Openings. 5th Annual Research Presentation Meeting on Concrete Engineering. : 201-204 (in Japanese).

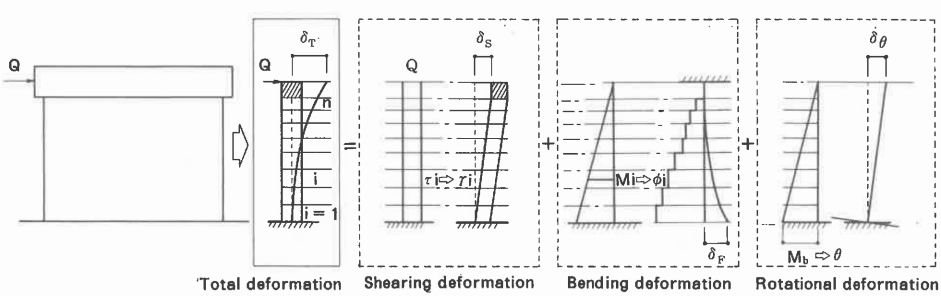

Fig. 1 Concept of the method to estimate deformation by discrete beam model

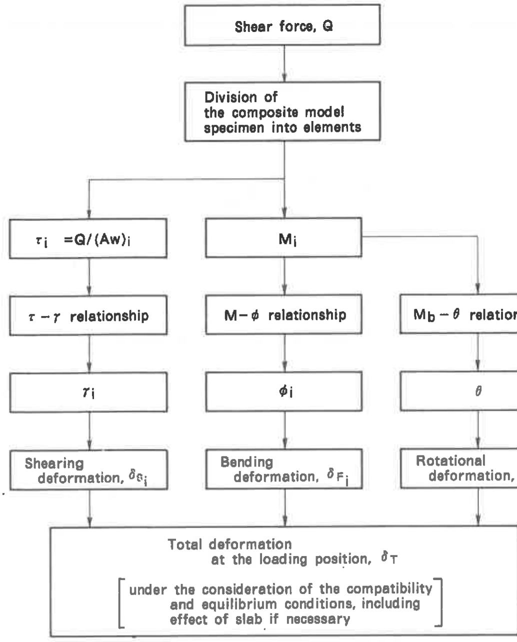

Fig. 2 Computational flow

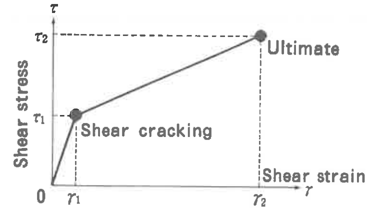

Fig. 3 $\tau-\gamma$ relationship model

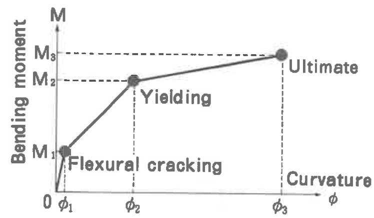

Fig. 4 M $-\phi$ relationship model

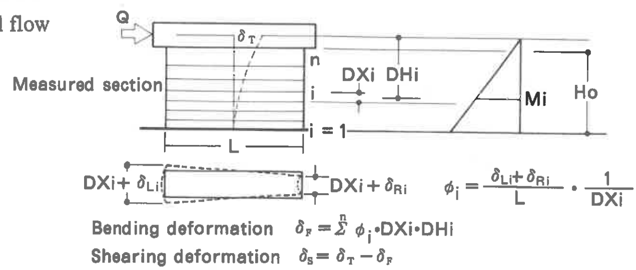

Fig. 7 Deformation separation method for test results

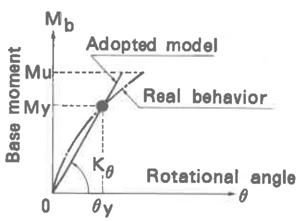

Fig. 5 M$_b$ $-\theta$ relationship model

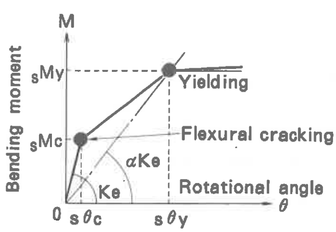

Fig. 6 M $-\theta$ relationship model for slab

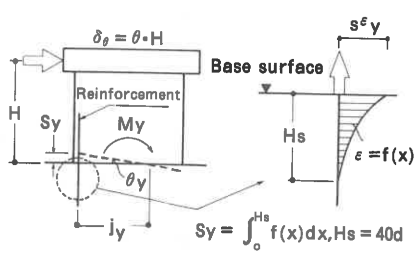

Fig. 8 Rotational deformation and strain distribution of embedded reinforcement at yielding stage

Table 1 Specimens evaluated

Test series	Specimen	Qty	Configuration
Series P1(PWR)	P1-1 to 9	9	box wall, cylindrical wall, octagonal tube wall
Series P2(PWR)	P2-4,5	2	thick-walled octagonal tube wall
Series B1(BWR)	B1-1 to 7	7	box wall
Series B2(BWR)	B2-1 to 7	7	cylindrical wall, truncated conical wall

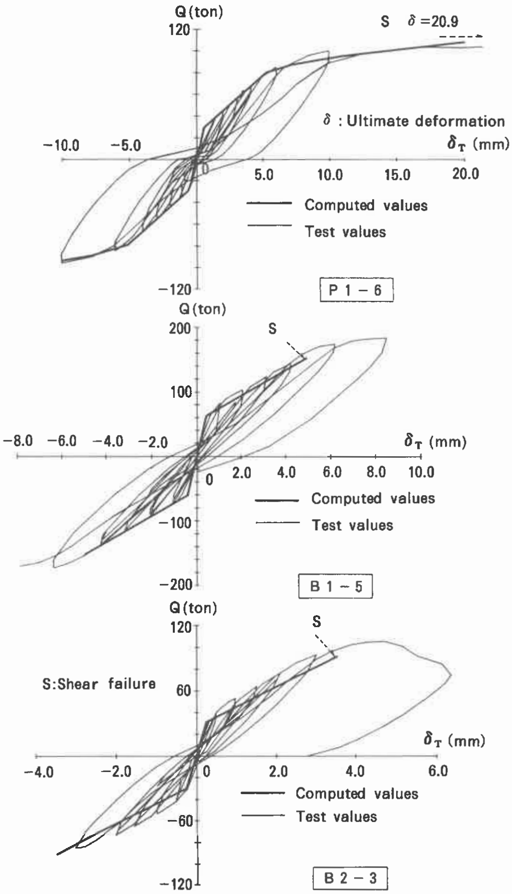

Fig. 9 Load-total deformation relationships of small-sized and partial model specimens

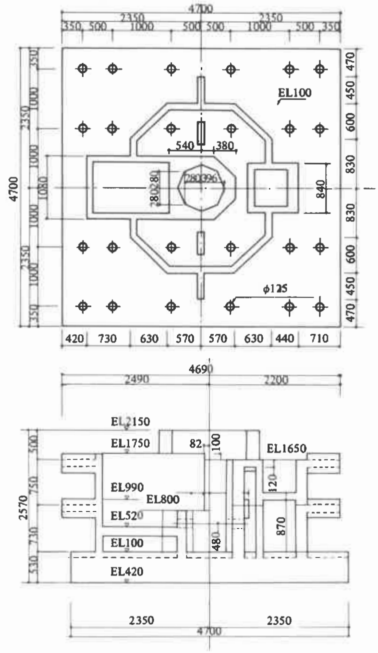

Fig. 10 Configuration of PWR type composite model specimen

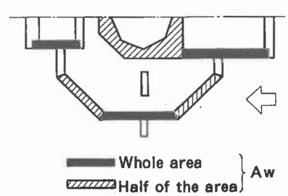

Fig. 12 Definition of the effective shear area of web (A_W)

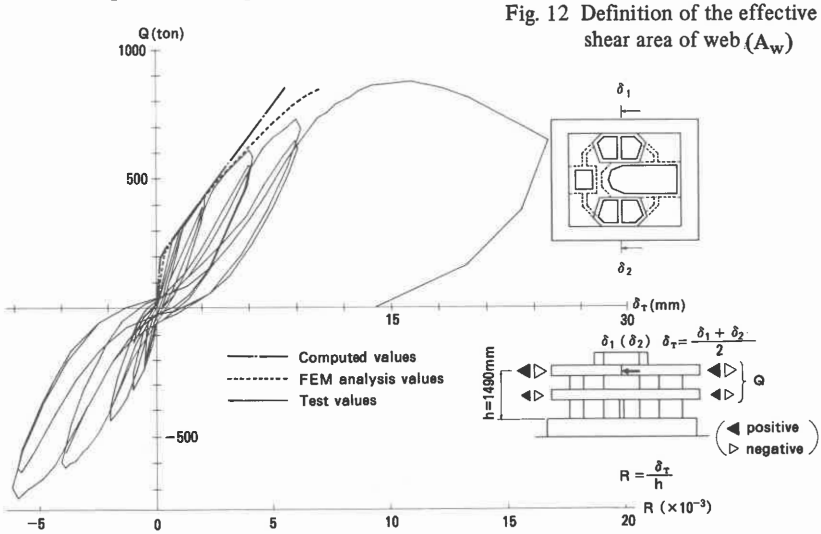

Fig. 11 Load-total deformation relationships of PWR type composite model specimen